Editorial Manager(tm) for Geosphere
Manuscript Draft

Manuscript Number: GS537R1

Title: Late Miocene Submarine Volcanism in the Ross Embayment, Antarctica

Short Title:

Article Type: Research Paper

Keywords: ANDRILL, AND1-B core, McMurdo Sound, submarine volcanism

Corresponding Author: Dr. Alessio Di Roberto, Ph.D.

Corresponding Author's Institution: Istituto Nazionale di Geofisica e Vulcanologia

First Author: Alessio Di Roberto, PhD

Order of Authors: Alessio Di Roberto, PhD; Massimo Pompilio, First Researcher; Thomas Wilch

Abstract: The ANDRILL McMurdo Ice Shelf (MIS) initiative recovered a 1285 m-long core (MIS AND-1B) composed of cyclic glacimarine sediments with interbedded volcanic deposits. By far the thickest continuous volcanic sequence is about 175 m long and is found at mid-core depths from 584.19 to 759.32 meters below sea floor (mbsf). The sequence was logged and initial interpretations of lithostratigraphic subdivisions were made on-ice during drilling in late 2006. Subsequent observations, based on image, petrographic, and SEM-EDS analyses, provide a more detailed, revised interpretation of a thick submarine to emergent volcanic succession.
The sequence is subdivided into two main subsequences on the basis of sediment composition, texture and alteration style. The ~70 m thick lower subsequence consists mostly of monothematic stacked volcanic-rich mudstone and sandstone deposits, which are attributed to epiclastic gravity flow turbidite processes. This subsequence is consistent with abundant active volcanism that occurred at a distal site with respect to the drill site. The ~105 m thick upper subsequence consists mainly of interbedded tuff, lapilli tuff, and volcanic diamictite. A late Miocene (6.48 Ma) 2.81 m-thick subaqueously emplaced lava flow occurs within the second subsequence. This second subsequence is attributed to recurring cycles of submarine to emergent volcanic activity that occurred proximal to the drill site. This new dataset provides 1) the first rock evidence of significant late Miocene submarine volcanic activity in the Ross Embayment during a period of no to limited glaciation , and 2) a rich stratigraphic record that elucidates submarine volcano-sedimentary processes in an off-shore setting.

*Cover Letter
Click here to download Cover Letter: Cover letter.doc

Late Miocene Submarine Volcanism in the Ross Embayment, Antarctica

Alessio Di Roberto[1], Massimo Pompilio[1], Thomas I. Wilch[2].

1 - Istituto Nazionale di Geofisica e Vulcanologia, sezione di Pisa, Via della Faggiola, 32-56126 Pisa, Italy.

2 - Department of Geological Sciences, Albion College, 611 E. Porter St. Albion, Michigan 49224.

ABSTRACT

The ANDRILL McMurdo Ice Shelf (MIS) initiative recovered a 1285 m-long core (MIS AND-1B) composed of cyclic glacimarine sediments with interbedded volcanic deposits. By far the thickest continuous volcanic sequence is about 175 m long and is found at mid-core depths from 584.19 to 759.32 meters below sea floor (mbsf). The sequence was logged and initial interpretations of lithostratigraphic subdivisions were made on-ice during drilling in late 2006. Subsequent observations, based on image, petrographic, and SEM-EDS analyses, provide a more detailed, revised interpretation of a thick submarine to emergent volcanic succession.

The sequence is subdivided into two main subsequences on the basis of sediment composition, texture and alteration style. The ~70 m thick lower subsequence consists mostly of monothematic stacked volcanic-rich mudstone and sandstone deposits, which are attributed to epiclastic gravity flow turbidite processes. This subsequence is consistent with abundant active volcanism that occurred at a distal site with respect to the drill site. The ~105 m thick upper subsequence consists mainly of interbedded tuff, lapilli tuff, and volcanic diamictite. A late Miocene (6.48 Ma) 2.81 m-thick subaqueously emplaced lava flow occurs within the second subsequence. This second subsequence is attributed to recurring cycles of submarine to emergent volcanic activity that occurred proximal to the drill site. This new dataset provides 1) the first rock evidence of significant late Miocene submarine volcanic activity in the Ross Embayment during a period of no to limited glaciation , and 2) a rich stratigraphic record that elucidates submarine volcano-sedimentary processes in an off-shore setting.

INTRODUCTION

The ANDRILL (Antarctic Geological Drilling Programme) 1285 m-long AND-1B core provides a well-preserved (>98% core recovery) high-resolution, Late Neogene record from the near-shore glacimarine environment in Antarctica (Naish et al., 2007, 2009). The marine core was obtained from beneath the McMurdo Ice Shelf (MIS), in the Ross Embayment of Antarctica (Fig.

1). The MIS drill site is located about 10 km east of Hut Point Peninsula, Ross Island (Fig. 1), in the subsidence moat created by the volcanic Ross Island (Naish et al., 2007). The core top is situated 943 m below sea level. The core (Fig. 2) consists of intercalated glacigenic, biogenic, and volcanic deposits, which have been interpreted in terms of changing environmental conditions since 12 Ma (McKay et al., 2009; Naish et al., 2009). Volcanic rocks form a significant component of the core: more than 65,000 of the >2 mm clasts (70% of total clast count) are volcanic (Pompilio et al., 2007), abundant volcanic layers occur throughout the core with thicknesses ranging from mm to 175 m. This study focuses on the 175-m-long volcanic interval from 584.19 to 759.32 mbsf (meters below sea floor), which was classified in the initial report core log record as lithostratigraphic unit 5 (LSU5) by Krissek et al. (2007).

The AND-1B core stratigraphic sequence was initially subdivided into eight lithostratigraphic units (LSU1-8) composed of several depositional sediment facies. Among the eight, LSU5 (Fig.2) is distinctive on the basis of its high volcanic content, lack of diatomite, and varied range of siliciclastic sediments (Krissek et al., 2007). LSU5 includes different depositional facies whose products can be attributed to both reworked and primary volcanic depositional processes. Preliminary paleomagnetic studies of the AND-1B core carried out on-ice (Wilson et al., 2007b) revealed that LSU5 covers a time span of at least several hundreds of ka, as at least 5 inversions of the magnetic polarity occur in this interval. A 2.81-m-thick intermediate lava flow at 649.2-646.5 mbsf was dated to 6.48±0.13 Ma and provides the only isotopic age of the interval (Wilson et al., 2007c). Initial interpretations of the core were based solely on core logging done during drilling. Here we provide a more detailed and refined interpretation of LSU5, based on re-analysis of the original non-genetic core log descriptions and the actual core, as well as new analysis of accurate high-resolution digital images and petrographic thin sections. We describe and discuss primary subaqueous volcanic deposits as well as volcanic-rich epiclastic debris in LSU5 and examine facies relations within a vertical sequence. Interpretations of eruptive and depositional processes for both pyroclastic and epiclastic debris define the evolution of this thick volcaniclastic sequence. The 175-m-thick interval records intense subaqueous volcanic activity during a period of limited to no glaciation.

EREBUS VOLCANIC PROVINCE

The MIS AND-1B drill site is located in midst of the Erebus Volcanic Province (Fig. 1), which is comprised of alkaline Neogene volcanic centers on the west flank of the intra-continental

West Antarctic rift system in the McMurdo Sound region (Kyle, 1990). Ross Island, a large volcanic complex just north of the drill site, is dominated by the active 3794 m Mt. Erebus, surrounded radially by Mt. Terror, Mt. Bird and Hut Point Peninsula eruptive centers (Figure 1). Mt. Erebus is composed mostly of basanite and its fractionated product phonolite (Kyle, 1977, 1981; Kyle et al., 1992); the oldest Erebus outcrops are low elevation 1.3 Ma Cape Barne rock (Esser et al., 2004). Mt. Bird and Mt. Terror are basanitic shield volcanoes and erupted between 4.6–3.8 and 1.7–1.3 Ma, respectively (Wright and Kyle, 1990a and b; Kyle and Muncy, 1989). Hut Point Peninsula, located just 10 km west of the drill site, is the most proximal subaerial volcanic outcrop to the drill site. Surface mapping and drill core records from the 1970's at Hut Point Peninsula reveal a Pleistocene (since 1.3 Ma) record of evolving alkaline volcanism, dominated by basanitic-hawaiitic cinder cones and a phonolite dome at the surface (Kyle, 1981).

Major volcanic centers are also located south of the AND-1B drill site. White Island, whose magmatism dates back to 7.7 Ma, is a basanite to tephriphonolite shield volcano and is the next most proximal volcano, located 15 km SSE of the drill site (Cooper et al., 2007). Further to the south (40-60 km from the drill site), Black Island, Minna Bluff, Mount Morning and Mount Discovery are all major volcanic centers. The earliest known volcanic outcrops date back to 19 Ma and include extensive evolved alkaline explosive vent complexes on the northwestern and northeastern slopes of Mt. Morning and, farther south, at Mason Spur and Helms Bluff (Armstrong, 1978; Kyle and Muncy, 1989; Kyle, 1990). A thick pumice lapilli tuff, dated to 22 Ma, was also found in the Cape Roberts project CRP-2 drillhole (Armienti, et al., 2001; McIntosh, 2001). Late Miocene volcanism with ages similar to the ~6.5 Ma lava flow in LSU5 is known to have occurred at both White Island and Minna Bluff. Minna Bluff to the south of the drill site formed between 12 and 6 Ma and has since acted as an important barrier to the flow of the Ross Ice Shelf into McMurdo Sound (Wilch et al., 2008; Talarico and Sandroni, 2009). Glacial reconstructions show that flowlines of a grounded ice sheet in the Ross Embayment directed to the drill site would sweep around Minna Bluff (12-6 Ma) and past White Island (7.7– 0.2 Ma) (Naish et al., 2009). Two major glacial unconformities dated at ~10.4 and 9.6 Ma on Minna Bluff are attributed to erosion by an early Ross Ice Sheet (Fargo et al., 2008). Talarico and Sandroni (2009) suggested that clasts from both Minna Bluff and White Island are important components of glacial deposits in the AND-1B core.

Recent aeromagnetic studies have also suggested the possible existence of submarine volcanoes beneath the McMurdo Ice Shelf, as well as submarine lava flow extensions of exposed volcanic islands including White Island (Wilson et al., 2007a). These inferred submarine volcanoes have not been sampled or dated.

TECHNIQUES

The AND-1B core was logged first on-ice during the drilling in late 2006 (Krissek et al. 2007; Pompilio et al., 2007). Core description was conducted by the ANDRILL McMurdo Ice Shelf (MIS) sedimentology/stratigraphy team, following procedures and operations outlined in the Scientific Logistics Implementation Plan for the ANDRILL MIS Project (SLIP; Naish et al., 2006). Preliminary stratigraphic and petrologic data on volcanic rocks in the AND-1B core are reported in Krissek et al. (2007) and in Pompilio et al. (2007) and provide the starting point for analysis and interpretations in this study.

Additional macroscopic and stratigraphic descriptions of LSU5 have been further implemented by analysis of high-resolution digital images visualized in a desktop workstation using Corelyzer software (Rao et al., 2006). These images were studied in order to infer mechanisms of eruption, transport and deposition. Macroscopic observations of digital images and core were integrated with detailed sample characterization performed on more than 50 thin sections distributed within LSU5; additional sampling was undertaken where particular structures are evident or in correspondence to specific sedimentary units. Selected sample micro- and macro-textures were further analyzed using a SEM-EDS Philips XL30 scanning electron microscope (accelerating voltage 20 kV, beam current 1 nA, working distance 10 mm), equipped with energy dispersive X-ray analysis (EDAX DX 4) at the Earth Science Department of Pisa University and BSE images collected with a JEOL JXA 8200 Superprobe at INGV-Rome.

FACIES

Krissek et al. (2007) grouped primary and near-primary volcanic rocks and sediments in a single facies (designated #11 in core logs), which includes lapilli tuff, volcanic diamictite, and a tephritic lava flow. Some of these deposits were interpreted as slightly reworked by sediment gravity flow processes but less reworked than volcanic-rich equivalents of other facies. Volcaniclastic rocks were also included in primarily non-volcanic siliciclastic facies, including Facies #2 (Mudstone), #3 (Interstratified mudstone and sandstone), #4 (Mudstone with interdispersed common clasts), #5 (Rhythmically interlaminated mudstone with siltstone or sandstone) and #6 (Sandstone) (Krissek et al., 2007). Here, we redefine and redescribe these facies in the context of the LSU5 volcanic interval. On the basis of detailed stratigraphic, textural and component analyses we subdivided facies 11 into 3 sub-facies, (11a to c) keeping the same number for coherency (Table 1 and supplemental material); this further subdivision was considered necessary to detail the complex architecture of LSU5.

(Facies 2-6) Volcanic-rich mudstone to sandstone

We group the five facies (Facies 2, 3, 4, 5 and 6) identified by Krissek et al. (2007) as products of reworking of primary volcanic deposits into a single facies association. In the original facies description, these volcanic units were included as variations of facies that were mostly siliciclastic. The lower part of LSU5 is dominated by these facies, including dark grey to black, cm- to mm-thick beds of siltstone, clayey siltstone, and fine to medium grained sandstone, interlaminated and interbedded at millimeter to centimeter scales (Fig. 3A and supplemental material 1). Beds commonly exhibit normal grading, although non-graded massive beds also occur. Planar lamination and cross-stratification are common while ripple cross lamination is mostly limited to coarse siltstone. Incomplete Bouma sequences sometimes occur. Basal contacts with underlying sediments are either sharp or diffuse, whereas in the topmost part convolute bedding and fluid escape structures are also common.

Sandstone is less common and is mostly represented by volcanic fine- to medium-grained sandstone, which is normally graded to volcanic siltstone; some non-graded massive beds also occur. Incipient planar laminations, cross-stratification and climbing ripple laminations are common. Basal contacts of sandstone units are usually sharp and interpreted as erosional. The majority of beds are constituted by a heterolithic mix of volcanic-derived clasts (i.e. glass shards, variously vesicular pumices and scoria, dense lava fragments, and magmatic crystals) with variable and sometimes significant amounts of mainly basement-derived clasts (granitoids, metasediments) and mudstone intraclasts. Both volcanic-derived and crystalline rock fragments are subangular to well rounded and show traces of intense reworking by granule abrasion and comminution. Sandstone and siltstone are usually matrix-supported; the matrix is composed of silt-sized (tens of µm) volcanic fragments and minerals, clay aggregates and crystalline to microcrystalline zeolites.

(Facies 11a) –Lapilli Tuff and Tuff

Lapilli tuff and tuff (Fig. 3B and supplemental material 2) are one of the most widespread deposits within LSU5. The units are composed of cm- to dm-thick, massive to crudely stratified, coarse lapilli tuff to fine lapilli tuff (LT) (sizes after White, 2006) normally graded to or overlain by well-bedded, extremely fine to fine tuff (T) with diffuse parallel to low-angle cross laminations. The coarser LT beds are moderately to poorly sorted and are composed of juvenile greenish-yellowish colored clasts set in a dark green matrix; they are matrix- to clast-supported and sorting/bedding may be obscured by alteration, although normal grading is obvious in some units. The finer T beds are moderately to well sorted, commonly clast-supported and open-framework textured, and rarely graded. Juvenile fragments of both LT and T beds are composed of texturally homogeneous pumice, scoria and glass shards mixed with reduced amounts of igneous crystals, and dense, angular lava fragments. Abundant reddish oxidized fragments occur especially in the uppermost part of the sequence. Juvenile fragments are mostly aphyric, with few crystals of plagioclase, pyroxene, amphibole and altered olivine in a glassy matrix. Some juvenile fragments are tachylitic with abundant microlaths of plagioclase frequently altered and replaced by clay minerals and chlorite.

Within lapilli tuff, volcanic fragments are variably vesicular likely representing a continuum between end-members represented by clasts with low vesicularity made up of few relatively large vesicles (hundreds of μm in diameter) up to honeycomb-textured clasts with fine vesicles (few tens of μm in diameter). Vesicles are frequently convoluted and deformed with some clasts showing a probable vesiculation after fragmentation. In these clasts, early syneruptive vesiculation is preserved in vesicles aligned below quenched and fractured clast rims while post-fragmentation processes give rise to undeformed, mostly spherical vesicles, developed in the inner part of the clast. A large portion of fragments exhibit marginal quenching and widespread fracturing. The nature of the vesicularity and quenching, in addition to the presence of fluidal deformation of the thin glass tips, suggest possible heat retention during deposition.

Stratigraphic relationships between mainly massive LT and laminated fine T intervals are variable. Three main cases occur: i) deposits with similar proportion of LT and T (the most common); ii) much reduced portions of LT overlain by extensively developed fine T iii) multiple stacked sequences of LT overlain by, and separated by erosion surfaces from very limited occurrence of fine T. Laminated fine-grained T is frequently overlain by yellow-gray volcanic siltstone or claystone, which is moderately to intensely bioturbated with frequent convolution, fluid escape structures and load structures. Coarse T is usually cemented by a micritic to crystalline matrix made up by clay and zeolites (mainly analcime and phillipsite). Fine-grained T is always cemented by highly crystalline zeolite (phillipsite and analcime).

Few layers of parallel to low-angle laminated, extremely fine, well sorted tuff also occur just above the top of LSU5 at 584.19-584.84 mbsf. Although Krissek et al. (2007) ascribed these layers to LSU4.4, these tuffs can be considered genetically linked to similar deposits of LSU5. These tuff beds are cm- to dm-thick and clast-supported and are composed of y-shaped to blocky, poorly vesicular and aphyric glass shards. Calcite to zeolite crystalline cement constitutes the matrix. Many shards exhibit a few tens of μm-thick, concentric rims of devitrified glass and in some cases tiny perlitic fractures.

(Facies 11b) - Lava Flow

A 2.81 m-thick lava flow occurs within LSU5 sequence at 646.49 and 649.30 mbsf (Fig. 3C and supplemental material 3). The lava flow is a fine-grained tephrite, with few large (>1 mm) feldspar phenocrysts set in a pilotaxitic groundmass. The upper lava flow contact exhibits a 1-2 cm thick alteration rim, composed of a series of concentric rinds of calcite and zeolite. Similarly, the basal 2 cm of the flow in contact with underlying sediments are also altered to calcite, zeolite (Krissek et al., 2007) and pyrite. Soft-sediment deformation occurs at the contact between the lava flow and underlying muddy sediments. Abundant mm-wide fractures and sparse vesicles are evident within the lava and are now occupied by secondary calcite and silica veins and amygdales. Fractures near the top and base of the lava are generally parallel to the bounding surfaces; fractures in the core of the lava are inclined to anastamosing (Krissek et al., 2007). No clear evidences of pillow-like structures exist for this lava. The occurrence of glassy rinds, flow and shear textures and the presence of a subaqueous gravity flow just above the lava flow indicate a submarine setting (Pompilio et al., 2007).

(Facies 11c) - Volcanic Diamictite

Diamictite (Fig. 3D and supplemental material 4), in which volcanic detritus is dominant, is an important component of the LSU5 volcanic sequence and represents a variation of the heterolithic facies 9 (Stratified Diamictite) and 10 (Massive Diamictite) described by Krissek et al. (2007). Most of the volcanic diamictite is massive, very poorly sorted and very poorly to faintly bedded, although normal grading appears in some examples. The volcanic diamictites are composed by coarse sand- to pebble-sized clasts of dense, angular lavas with textures analogous to the lava flow, scoria and oxidized altered volcanics enclosed in a clay- to sand-sized matrix. Some lava clasts have a ‘jig-saw’ texture suggesting short transport after breakage; accidental very rounded, yellow claystone intraclasts also occur.

The volcanic diamictite matrix is dark green colored and dominantly composed of clay- and zeolite-altered volcanic ash. Volcanic diamictite beds are usually less than 2 m thick (Krissek et al., 2007) but up to 10 m-thick sequences of stacked diamictite beds also occur.

STRATIGRAPHY OF AND-1B - LSU5

We report here observational data collected off-ice, including examination of high resolution images of the core and analysis of thin sections by optical and scanning electron microscope. This information integrates and expands upon previous on-ice core descriptions summarized in Krissek et al. (2007). The LSU5 was originally subdivided on-ice by the AND-1B sedimentology team into

4 subunits, LSU 5.1-5.4, that were differentiated on the basis of lithostratigraphic characteristics. Here we simplify the model and subdivide the entire LSU5 into two sequences i.e. Sequence LSU5A and Sequence LSU5B, on the basis of volcanic and sedimentologic facies analysis.

Sequence LSU5A (759.32-688.92 mbsf - LSU5.4)

Sequence LSU5A includes the whole of LSU5.4 of Krissek et al. (2007) and extends from 759.32 to 688.92 mbsf. It is constituted by an almost monothematic sequence of siltstone, clayey siltstone and sandstone belonging to facies 2, 3, 4, 5 and 6 of Krissek et al. (2007). Beds are volcanic-rich throughout LSU5A, with variable quantities of non-volcanic, mainly crystalline rock fragments. Crystalline rock fragments are more abundant in some layers in the lowermost meters of the subsequence (e.g., in the volcanic-rich, clast-rich muddy diamictite located at 750.54-751.01 mbsf;). Siltstone, clayey siltstone and sandstone are periodically interrupted by yellowish, mm- to cm-thick laminae enriched in biogenic silica sediments. Bioturbation is variable and sometimes masked by sediment cementation.

In the uppermost part of LSU5A (714.80-688.92 mbsf), cm- to dm-thick beds of lapilli tuff and tuff (facies 11b) are interfingered with laminated sandstone and siltstone. The progressive increase in the number and thickness of tuff beds towards the top of sequence LSU5A marks the transition into sequence LSU5B. The passage from sequence LSU5A to sequence LSU5B is not marked by a sharp unconformity, hiatus or erosive surface and was put at 688.92 mbsf since above this depth tuff beds became predominant.

Sequence LSU5B (688.92–584.19 mbsf - LSU5.3 - 5.1)

Sequence LSU5B comprises three of the lithostratigraphic subunits (LSU5.1-5.3) traced by Krissek et al. (2007), as well as the lowest 2 meters of LSU4.4. The sequence extends from 688.92 to 584.19 mbsf and is largely composed by stacked tuff and lapilli tuff beds (facies 11a) and volcanic diamictite (facies 11c). Up to several meter-thick intervals of interleaved volcanic-rich sandy claystone and dark sandstone (Facies 3,4,5; e.g., between 618.58-608.22 mbsf) also occur. Deposits consist of dark olive to grey sandy claystone beds, up to 1 m-thick, interfingered with mm- to cm-thick sandstone, laminated to massive and frequently bioturbated, though the dark color may obscure the degree of bioturbation present.

The sequence also includes the 2.81 m-thick lava flow (Facies 11b) found from 646.49 to 649.30 mbsf. The lava flow is associated with incipiently bedded, very poorly sorted and crudely normally graded volcanic diamictites (Facies 11c). Volcanic diamictites, up to ~8 m-thick, are widespread in the sequence even when not associated with a lava flow (ex: 674.83-683.13, 658.41-655.45, and 620.50-618.93 mbsf).

Very close to the topmost part of the sequence (584.19-584.84 mbsf) several stacked extremely fine tuff layers occur (Facies 11b); they are almost completely composed of well sorted, y-shaped to blocky glass shards with traces of glass hydration, slight glass rim leaching and pervasive cracks. The deposit is clast-supported and cemented with crystalline calcite.

FACIES INTERPRETATIONS

Rationale

Submarine, non-welded pyroclastic debris that are directly related to volcanic explosions are very difficult to discriminate from cold, remobilized, volcanogenic mass flow deposits because of the lack of unequivocal distinctive criteria. The distinction is more difficult where deposits are altered, metamorphosed and/or deformed as in ancient sequences or where sediment exposure is laterally limited and depositional structures are poorly traceable. Notwithstanding, a number of recent works have demonstrated that discrimination of submarine primary pyroclastic deposits from those subjected to reworking and redeposition (epiclastic) is possible where detailed facies analysis is performed (White, 1996; Skilling, 1994; Smellie and Hole, 1997; Mueller et al., 2000). Moreover the nature, texture and morphological properties of clasts can be used to help in discriminating the sediment origin.

Basaltic eruptions at shallow to moderate depths, such as those observed at Surtsey Volcano, Iceland (Kokelaar, 1983), Falcon Island, Tonga (Hoffmeister et al., 1929), Capelinhos, Faial Island, Azores (Machado et al., 1962; Cole et al., 1996, 2001; Solgevik et al., 2007; Zanon et al., 2008), Kick'em-Jenny (Lesser Antilles) and the recent eruption off the coast of Nuku'alofa, Tonga (Associated Press, 2009), produce great amounts of fragmental volcanic products. Volcanic rock and detritus can be transferred to the basins either by eruptive or syneruptive processes like subaqueous pyroclastic flows and eruption-fed aqueous density currents Alternatively, volcanic material temporarily stored on the cone flanks can be redistributed into adjacent basins via gravity flows.

Primary basaltic volcaniclastic deposits produced by recent and ancient mafic underwater eruptions, such as at Greenland (Mueller et al., 2000), are typified by a very homogeneous (monomictic) composition and dominated by a poorly sorted mixture of mafic scoria fragments, glass shards and crystals. The angular clasts preserve primary fragile structures (e.g., thin glassy rims) and are unabraded. Epiclastic or reworked volcanic-rich deposits, not directly related to a single eruption, may originate from either subaerial pyroclastic sediments or from submarine volcanic flows. Such reworking occurs in particular during periods of quiescence of the eruptive activity. Primary pyroclastic deposits may be eroded and transported by fluvial, marine and glacial systems. Volcanic fragments occurring in epiclastic deposits usually show traces of intense reworking such as rounding, abrasion and comminution and are variably mixed with non-volcanic material from within the depositional basin itself, or derived from source rocks that lie outside the basin area, including siliciclastic and crystalline basement rocks and/or bioclastic fragments. Lithological and sedimentological observations indicate that both epiclastic and primary volcaniclastic deposits occur throughout LSU5 and provide a record of an evolving submarine volcanic complex.

Sequence LSU5A - 759.30 - 688.92 mbsf

A combination of sedimentary structures, including bedding, planar and low-angle cross-stratification, normal grading, partial Bouma sequences, convolute bedding, and rip-up clasts, indicates a turbidity current origin for the majority of sequence LSU5A. Among turbidites, the dominance of heterolithic siltstone, silty claystone and sandstone, as well as intense reworking of clasts all point to a prevalent epiclastic origin of sediments. Turbidites may be deposited by turbidity currents resulting from grounding-line fan processes or volcanic/tectonic activity. The fine nature of the sediment and the near total absence of dropstones indicate that turbidity currents may develop from a grounding line located far from the drill site and may funnel fine-grained products produced by fluvial and glacial erosion of volcanic and basement rock. Similar deposits may be produced either from the mixing of primary submarine volcanic deposits with non-volcanic detritus; the mixing may occur both prior to or during the transport towards the deeper portion of the sedimentary system with the non-volcanic fractions supplied by glacier tongues descending from the Transantarctic Mountain front and by grounding line processes.

In the upper part of the LSU5A sequence, a significant change in depositional environment and processes occur. The presence of lapilli tuff and tuff in the upper meters of sequence LSU5A marks transition from the predominantly epiclastic sedimentation to a system dominated by materials directly derived from explosive volcanic activity. Though core exposure is limited, the tuff and lapilli tuff deposits are similar to eruption-fed density current deposits described by several authors in recent or ancient submarine and subglacial explosive volcanic successions in several location (e.g. Fiske, 1963; Mueller and White, 1992; White, 1996; Smellie and Hole, 1997; Fiske et al., 1998; Smellie, 1999; White and Houghton, 1999; White, 2000).

Poorly sorted and massive to crudely stratified lapilli tuff may represent the main body of highly concentrated, eruption-fed, aqueous density currents with high sedimentation rate, whereas the thin bedded and parallel to low-angle, cross laminated uppermost part of the tuff may represent deposition by co-genetic low density flows (White, 2000; Mueller, 2003). These low density flows may develop in the tail of the eruption-fed aqueous density currents (Kokelaar and Busby, 1992, Martin and White, 2001, Mueller, 2003) or by the collapse of fine sediments injected into the water column by subaqueous pyroclastic jets (the same that generate eruption-fed density currents) (Cashman and Fiske, 1991). The final drape may produce a very fine ash deposit elutriated from the main part of the flow during the transport (Mueller, 2003) and deposited as fall-out through the water column.

The interpretation of a primary volcanic density flow origin for these deposits is based on several key features, including the occurrence of very homogeneous components (scoria and dense lava fragments), the almost complete absence of grain abrasion and the complete preservation of clasts with complex shapes (Doucet et al., 1994; White, 2000). The evidence for heat retention associated with larger clasts during their deposition, i.e. marginal quenching, flattened and convoluted vesicles, and deformation of thin glass tips, supports the hypothesis of a primary deposition of syneruptive hot gravity flows. The presence of sparse tuff in the uppermost part of LSU5A indicates the initiation of sporadic explosive subaqueous activity close to the drill site. The limited thickness and small grain size of these deposits as well as their intermittent occurrence within the LSU5A sequence suggest that they resulted from either low-energy eruptive activity or a distal volcanic source (Song and Lo, 2002, Allen et al., 2007).

Sequence LSU5B - 688.92 – 584.19 mbsf

Sequence LSU5B, the upper sequence, represents a fundamental change in the sedimentary system both in terms of the nature and source of sediments, as well as the main depositional processes. The base of sequence LSU5B is not marked by a sharp unconformity, hiatus or erosive surface and was placed at 688.92 mbsf because at this depth coarse tuff beds begin to dominate. Lapilli tuff and tuff that comprise most of the second sequence resemble tuff couplets described in the upper part of sequence A, although the latter are characterized by thicker beds and coarser clast size. We attribute the bulk of the LSU5B succession to submarine explosive activity. Coarser grain size, bed thicknesses, and increase in frequency of lapilli tuff suggest an increase of explosive energy or a shift to an eruptive vent closer to the drill site.

A key volcanic feature in the core is the 2.81 m-thick lava flow (646.49 to 649.30 mbsf). The quenched rims on the flow, the presence of soft-sediment deformation at its base, and the analysis of bounding facies suggest that the lava flow was emplaced in a subaqueous environment. According to Walker's (1973) model, a subaerial tephritic (basaltic) lava flow with thickness similar to that cored, should be fed by a vent located within 4 km from the drill site. Considering that the emplacement in water implies a higher cooling rate and several other processes that promote higher viscosity and shorter lengths, the distance of 4 km for the vent position should be considered as maximum

Despite its own relevance and significance as a time stratigraphic horizon, the occurrence of lava offers a context for interpretation of the volcanic diamictites that are in contact with this coherent flow and are also found at various stratigraphic levels in LSU5B. As described above, the volcanic diamictite is composed of juvenile lava clasts that are texturally identical to the lava flow and by pumiceous fragments similar to those comprising the tuff. We interpret these diamictites as a mixture of clasts derived from autoclastic processes acting on the lava flow and clasts derived by the subaqueous explosive activity associated with the emplacement of a submarine lava flow. High-density mass flows (debris flows) related to cycles of growth and collapse of a local volcanic pile may develop in front of the lava flow so that volcanic diamictites may be found both at the base as well as above it. The presence of diamictites without related lava flows is attributed to the higher mobility of mass-flows compared to lava flows. Thus diamictites are proxies for lava flows that didn’t reach the drill site.

A continuum exists between processes that led to the formation of eruption-fed density current deposits and lava flows; thus, these processes and resultant processes may represent different phases of the same eruption depending upon the rate of extrusion and volatile content of the magma. Eruptive activity was intermittent and likely initiated by high eruption rates and high volatile contents that favor submarine fire fountaining or subaqueous pyroclastic jets which were transformed into eruption-fed density currents. During the late stages of these explosive eruptions lower eruption rates and diminished volatile content may produce lava flows and their associated diamictites (Stix and Gorton, 1989).

The abundant reddish, oxidized fragments in lava-related diamictites and in tuffs suggest thermal oxidation conditions of high-temperature volcanic materials (Cas and Wright, 1987; Song and Lo, 2002). Oxidizing conditions can be reached either during the emergence of the volcanic vent above sea level or if the eruptive plume (or fountain) reaches and breaks the sea surface; in this sense reddish, oxidized volcanic fragments may indicate the passage from a submarine eruptive environment to a shallow to emerging volcanic vent or eruption column. Further evidence of the emergence of the volcanic vent is the occurrence of stacked beds of extremely fine tuff, likely produced by contact of a vesiculating, ash-producing melt with external water, in the uppermost part of the LSU5B (584.19-584.84).

The presence of volcanic edifices close to the drill site was hypothesized by Wilson et al. (2007a) on the basis of presence of large accumulation of magnetic-susceptible detritus surrounding small (1–2 km wavelength), discrete, circular anomalies south of Hut Point Peninsula (Fig. 5).

The presence within the volcanic sequence of intervals composed of bioturbated, olive green to yellowish volcanic-rich epiclastic claystone interstratified with volcanic-rich epiclastic sandstone (Facies 11a; ex.: 618-608 mbsf) indicates that volcanic activity was periodically interrupted by periods of quiescence. During these periods the supply of volcaniclastic detritus was reduced and the deposition of epiclastic and hemipelagic sediments and of the benthic biologic activity (bioturbation) was conversely favored. A representation of the depositional system is schematized in Fig. 6.

DISCUSSION

Temporal evolution of the volcanic complex in LSU5

A well-constrained chronology has been developed for the AND-1B core from a combination of $^{40}Ar/^{39}Ar$ ages, microfossil biostratigraphy, correlation of magnetic polarity stratigraphy with the geomagnetic polarity time scale on primary volcanic deposits for about the first 600 m of AND-1B core (Wilson et al., 2007c, Naish et al., 2008). The age model considers the presence of several hiatuses, changes in accumulation rate between hiatuses and the presence of several erosion surfaces. Despite the paucity of volcanic material suitable for radiometric dating, the recognition of four well-defined time stratigraphic windows into the history and dynamics of the Ross Ice Shelf (Naish et al., 2008, Naish et al., 2009) had resulted. Age of ~4.9-4.6 Ma and ~3.6-3.2 Ma were indicated for 600-460 mbsf and 440-280 mbsf respectively, whereas ages of ~2.75-2.35 Ma and ~0.78-0.1 Ma were attributed to 253-150 mbsf and 80-20 mbsf (Naish et al., 2008, 2009). The chronology of LSU5 is weakened by the absence of biostratigraphic data below 586 m and the fact that correlation with the geomagnetic polarity time scale is relatively unconstrained.

The Miocene/Pliocene boundary should occur within a series of hiatuses in LSU5 between 615.50 and 635.00 mbsf (~620 mbsf) that account for ~1 Ma of time (Wilson et al., 2007c). A $^{40}Ar/^{39}Ar$ age (6.48±0.13 Ma) on the basaltic lava flow sampled at 648 mbsf indicates a late Miocene age for this interval of the core. The only chronostratigraphic data available below 700 mbsf are some $^{40}Ar/^{39}Ar$ ages of volcanic clasts affording maximum depositional ages of 9.41 Ma at 796.53 mbsf, 8.53 Ma at 822.78 mbsf and 13.57 Ma for the base of the AND-1B drill core (Ross et al., 2007 and personal communications). Thus lacking any other biostratigraphic constraints LSU5 volcanism initiated after 8.53Ma and ceased by 4.9 Ma. Additional, more detailed, clast-dating may refine the chronology of the lower half of the core, constraining the very beginning of the volcanic activity recorded in LSU 5.

Considering the drill site position, the LSU5 sequence may be an expression of the presently eroded and submarine north-westernmost extension of the 7.65±0.69 Ma White Island volcanic complex (Cooper et al., 2007, Wilson et al., 2007a). The general lack of siliciclastic glacial deposits and biogenic sediments interleaved with volcanic detritus is consistent with LSU5 representing a short-lived interval. On the other hand, the occurrence of more than one paleomagnetic reversals within this LSU place some minimum constraints (i.e. 100's ka) on the duration of volcanism (Wilson et al., 2007c).

Structural evolution of the volcanic complex in LSU5

The onset of the LSU5 volcanic sequence represents a significant shift from a glacier-dominated to a volcano-dominated geological system. Lithostraphic unit 6 (LSU6), which underlies LSU5 and extends to about 1225 mbsf, contains no pure volcanic horizons (Krissek et al. 2007). The activation of a new source of volcaniclastic material is indicated by the constant supply of very fine primary pyroclasts that were remobilized, reworked and form the volcanic fraction of the distal epiclastic turbidites recovered from the lowermost part of sequence LSU5A. The first evidence of a nearby growing volcanic complex in the McMurdo Sound basin and in LSU5 is the eruption-fed aqueous density current deposits that are interlayered with laminated volcanic claystone and siltstone in the uppermost part of sequence LSU5A.

Sequence LSU5B may have resulted from an increase of eruptive energy due to higher magma supply or gas content, and/or a shift of the eruptive activity closer to the drill site. Eruptions may have been produced by very complex edifices made up of several monogenetic and closely spaced and often overlapping cones; similar structures were produced during recent basaltic eruption at many locations, including Surtsey and its associated satellites (Thorarinsson, 1964; Lorenz, 1974; Jakobsson and Moore, 1982; Kokelaar and Durant, 1983), Falcon Island, Tonga (Hoffmeister et al., 1929), and Capelinhos or São Roque volcano Azores (Machado et al., 1962; Cole et al., 1996, 2001; Solgevik et al., 2007; Zanon et al., 2008). Similar volcanic complexes have also been inferred from ancient volcanic sequences like Lookout Bluff, New Zealand (Maicher, 2003), Pahvant Butte, Utah (White, 1996; 2001) and Kangerluluk sequence, southeast Greenland (Mueller et al., 2000, 2002).

Our interpretations of facies associations in LSU5 suggest that a single eruption (or eruptive period) started with a high energy phase with the deposition of lapilli tuff and tuff, followed by effusive emission of lava flows and related volcanic diamictites when the energy or gas content decreased. Single eruptive events were likely short-lived, with activity commonly lasting from days to a few years. Observations at Surtsey and Capelinhos indicate that eruptions lasting several days to a few weeks constructed edifices as big as 180 m above the sea level (>300 m above seafloor) (Thorarinsson et al., 1964, Machado et al., 1962). Analogous to these observed eruptions, the LSU5 activity could have been cyclical, intermittent and alternating with quiescent periods during which erosion of primary volcanic deposits and deposition of epiclastic turbidites occurred. The growth of the volcanic complex may have continued until the emergence of the volcanic complex or until the establishment of a very shallow water setting, as testified by high temperature oxidization products that are abundant in the sequence.

In the topmost part of the sequence LSU5B, a series of hiatuses occur mainly within volcanic-rich epiclastic deposits (wavy dashed red line in Fig. 2) indicating that volcanic activity was repeatedly interrupted by variably long periods of quiescence. During quiescence, erosion of volcanic deposits and epiclastic deposition occurred. The duration of these periods of reduced volcanic activity can’t be exactly constrained since biostratigraphic data are absent in this part of the core and correlation with geomagnetic polarity time scale is poorly constrained. However, an overall duration of ~1 Ma of time was reconstructed on the basis of stratigraphic considerations and geochronologic data (Wilson et al., 2007c).

Paleoclimatic and paleoenvironmental implications

Facies analysis and interpretation of LSU5 provide important data for paleoclimate and paleoenvironment reconstructions. Sequence LSU5A is bounded at its base by deposits that indicate subglacial conditions with oscillation of the grounding line and variable influence of icebergs in sediment delivery (LSU6 and 7). According to Krissek et al. (2007) these oscillations were accompanied by high sedimentation rates with submarine outwash and mass-flow deposition. The contact between LSU6 and LSU5 represents the onset of a long period of ice retreat from the AND-1B core site. The retreat is coincident with a rapid reduction to zero in out-sized clast (dropstone) abundance of both volcanic and Transantarctic Mountain basement origin that is observed in LSU5A (Talarico and Sandroni, 2009). The volcanic record of LSU5 is unusual in the context of the MIS AND-1B succession in that evidence for interruptions by glaciations is absent.

We infer open water conditions at the time of the volcanic eruptions documented in LSU5B. The emergence of a submarine volcano or generation of subaqueous pyroclastic jets that break the water surface preclude significant ice cover. During terrestrial subglacial eruptions the heat is more or less efficiently transferred from the erupted magma to the surrounding glacier (55->80%;

Höskuldsson and Sparks, 1997; Gudmundsson, 2003; Gudmundsson and Cook, 2004, Gudmundsson et al., 2004) while warm water derived from ice melting remains confined in a water-filled cavity in the glacier until it can escape through fractures or permeable ice layers. If an eruption persists, the subglacial volcano can break the ice surface and emerge, melting as much as several hundreds of meters of ice (Höskuldsson and Sparks, 1997). By contrast, in submarine eruptions the heat transfer to the overlying ice is likely much less efficient since a significant part of magma heat is lost during the interaction with seawater and the water eventually produced by ice-melting quickly cools and moves away. The presence of a thick ice shelf would likely prevent the emergence of the volcano and favor exclusively subaqueous activity. Thus a deglaciated condition above the drill site seems more realistic for the primary volcanic sequences of LSU5B. The lack of dropstones and glacial diamictite in LSU5 support this interpretation.

These considerations seem to be in agreement with data on marine oxygen isotope ($\delta^{18}O$) records from diatomite deposits overlying LSU5 that indicate higher global surface temperatures relative to today, with open-water conditions or thin ice cover in the Ross Embayment following the deposition of the volcanic sequence (Naish et al., 2009). As mentioned above, the volcanic activity may have continued up to the emergence of the volcanic complex as testified by abundant oxidized volcanic fragments both in tuff and in volcanic diamictite deposits.

The hypothesis of an emerging volcano seems at first appearance to be unrealistic in light of the current basin bathymetry and considering an eruptive style as that inferred by the sequence interpretation (Surtseyan style). Today, a volcano erupting on the seafloor, close to the AND-1B would need to grow vertically ~1000 m to be in shallow water or an emergent environment. However, the present basin configuration is the result of the loading of the crust by the Ross Island volcanic pile that produced ~1 km of subsidence beneath Ross Island and the development of an enclosing moat (Stern et al. 1991) superimposed on the regional pattern of accommodation space created by Late Cenozoic rifting (Naish et al. 2007). At the time that LSU5 deposition began, the Ross Island volcanic complex was most likely not present as the oldest outcrops at Mt. Bird are 4.6 Ma (Wright and Kyle, 1990a), and Mt. Erebus, comprising the bulk of the island, is younger than 1.3 Ma. If Ross Island were absent during the LSU5 deposition, then only regional subsidence related to the Late Cenozoic rifting was responsible for the basin configuration. Thus removing the ~1 km of subsidence beneath Ross Island a shallow water or emerged setting for the volcanic complex that produced LSU5B is consistent with what is known of regional subsidence history.

CONCLUSIONS

In summary, the new detailed volcano-stratigraphic data and interpretations of the thick and very complex volcaniclastic sequence in the AND-1B core provide new insights into the volcanic history and evolution of Erebus Volcanic Province during the Late Miocene. This study presents a record and a model of submarine volcanism in the intracontinental rift setting of the Ross Embayment. The study of LSU5 volcanic sequence enabled us to identify mechanisms of transport and deposition of volcaniclastic detritus during a time of minimal ice cover followed by the development of a new volcanic complex prior to 6.48 Ma. This volcanic complex began erupting in a submarine conditions and continued until the volcanic complex summit grew into a very shallow water environment. According to our interpretation, eruptive dynamics were similar to those characterizing recent shallow-water basaltic eruptions that are observed in several geologic settings. The sequence was probably deposited during repeated short-lived eruptive events; each event likely started with a high-energy phase during which the deposition of lapilli tuff and tuff occurred, followed by effusive emission of lava flows and related volcanic diamictites and other gravity flow deposits. More generally, the analysis of LSU5 volcanic sequence in AND-1B core furnishes a new and consistent dataset for the study of basaltic submarine volcanic activity and its products. Finally, the facies analysis and interpretation of LSU5 volcaniclastic sequence preclude any interaction with grounded or ungrounded ice indicating prevalent open water conditions (or at maximum seasonal sea ice).

ACKNOWLEDGMENTS

The ANDRILL project is a multinational collaboration between the Antarctic programs of Germany, Italy, New Zealand and the United States. Antarctica New Zealand is the project operator and developed the drilling system in collaboration with A. Pyne. Antarctica New Zealand supported the drilling team at Scott Base; Raytheon Polar Services Corporation supported the science team at McMurdo Station and the Crary Science and Engineering Laboratory. The ANDRILL Science Management Office at the University of Nebraska-Lincoln provided science planning and operational support. The scientific studies are jointly supported by the US National Science Foundation, the New Zealand Foundation for Research Science and Technology, the Italian Antarctic Research Programme, the German Research Foundation and the Alfred Wegener Institute for Polar and Marine Research. We are grateful for the detailed core-logging by the MIS Sedimentology Team and for helpful discussions with Phil Kyle during the drilling. We will also thank co-chiefs (Tim Naish, Ross Powell) and staff-scientist Richard Levy for coordinating efforts. We are also indebted to A. Cavallo (INGV-RM) for assistance in SEM observations ADR benefitted from a PNRA post-doc fellowship.

REFERENCES CITED

Allen, S.R., Hayward B.W. and Mathews E., 2007, A facies model for a submarine volcaniclastic apron: The Miocene Manukau Subgroup, New Zealand, Geological Society of America Bulletin, v. 119, p. 725-742; doi: 10.1130/B26066.1

Armienti, P., Tamponi, M. and Pompilio, M., 2001, Sand provenance from major and trace element analyses of bulk rock and sand grains from CRP-2/2A, Victoria Land Basin, Antarctica. Terra Antarctica, v. 8, p. 569-582.

Armstrong, R.L., 1978, K-Ar dating: Late Cenozoic McMurdo Volcanic Group and Dry Valley glacial history, Victoria Land, Antarctica. New Zealand Journal of Geology and Geophysics, v. 21, p. 685-698.

Associated Press, 2009, March 19, Tongan inspectors head to undersea volcano.

Cas R.A.F. and Wright J.V., 1987, Volcanic Successions, Allen and Unwin, London, 528 p.

Cashman, K.V. and Fiske, R.S., 1991, Fallout of pyroclastic debris from submarine volcanic eruptions. Science v. 253, p. 275-280.

Cole, P.D, Guest, J.E., and Duncan, A.M, 1996. Capelinhos: the disappearing volcano. Geology Today, v. 12, p. 68-72.

Cole, P.D., Guest, J.E., Duncan A. and Pacheco, J.M., 2001. Capelinhos 1957–1958, Faial, Azores: deposits formed by an emergent Surtseyan eruption, Bulletin of Volcanology, v. 63, p. 204-220.

Cooper, A.F., Adam, L.J., Coulter, R.F., Eby, G.N., and McIntosh, W.C., 2007, Geology, Geochronology and geochemistry of a basanitic volcano, White Island, Ross Sea, Antarctica. Journal of Volcanology and Geothermal Research, v. 165, p. 189-216.

Doucet, P., Mueller, W., and Chartrand, F., 1994, Archean, deepwater, volcanic eruptive products associated with the Coniagas massive deposit, Quebec, Canada, Canadian Journal of Earth Sciences, v. 31, p. 1569-1584.

Esser, R. P., Kyle, P.R. and McIntosh, W.C., 2004, $^{40}Ar/^{39}Ar$ dating of the eruptive history of Mt. Erebus, Antarctica: volcano evolution, Bulletin of Volcanology, v. 66, p. 671-686.

Fargo, A.J., McIntosh, W.C., Dunbar, N.W., and Wilch, T.I. 2008, $^{40}Ar/^{39}Ar$ Geochronology of Minna Bluff, Antarctica: Timing of Mid-Miocene Glacial Erosional Events Within the Ross Embayment, American Geophysical Union Fall Meeting, San Francisco, CA, Dec. 14-20.

Fiske, R. S., 1963, Subaqueous pyroclastic flows in the Ohanapecosh Formation, Washington. Geological Society of America Bulletin, v. 74, p. 391-406.

Fiske, R. S., Cashman, K. V., Shibata, A. & Watanabe, K., 1998. Tephra dispersal from Myojinsho, Japan, during its shallow submarine eruption of 1952-1953. Bulletin of Volcanology, v. 59, p. 262-275.

Gudmundsson, M.T., 2003, Melting of ice by magma–ice–water interactions during subglacial eruptions as an indicator of heat transfer in subaqueous eruptions, *in* White, J.D.L, Smellie, J.L., and Clague, D.A., eds., Explosive Subaqueous Volcanism American Geophysical Union Monograph v. 140, American Geophysical Union, Washington D.C., p. 61–72.

Gudmundsson, M.T. and Cook, K. 2004, The 1918 eruption of Katla, Iceland: Magma flow rates, ice melting rates and generation of the greatest jökulhlaup of the 20th century, General Assembly 2004, International Association of Volcanology and Chemistry of the Earth's Interior, Puco´n, Chile, 14-19 November.

Gudmundsson, M.T., Sigmundsson, F., Björnsson, H. and Högnadóttir, Th., 2004, The 1996 eruption at Gjálp, Vatnajökull ice cap, Iceland: efficiency of heat transfer, ice deformation and subglacial water pressure, Bulletin of Volcanology, v. 66, p. 46-65.

Hoffmeister, J. E., Ladd, H. S., and Ailing, H. L., 1929, Falcon Island, American Journal of Science, v. 18, p. 461-71.

Höskuldsson, A. and Sparks, R.S.J., 1997, Thermodynamics and fluid dynamics of effusive sub-glacial eruptions. Bulletin of Volcanology, v. 59, p. 219-230.

Jakobsson, S.P., and Moore, J.G., 1982, The Surtsey Research Drilling Project of 1979, Surtsey Research Progress Report, v. 9, p. 76-93.

Kokelaar, B.P., 1983, The mechanism of Surtseyan volcanism, Journal of the Geological Society of London, v. 140, p. 939-944.

Kokelaar, B.P. and Durant, G.P., 1983, The submarine eruption and erosion of Surtla (Surtsey), Iceland, Journal of Volcanology and Geothermal Research, v. 19, p. 239-246.

Kokelaar, B.P. and Busby, C., 1992, Subaqueous explosive eruption and welding of pyroclastic deposits. Science, v. 257, p. 196-201.

Krissek, L., Browne, G., Carter, L., Cowan, E., Dunbar, G., McKay, R., Naish, T., Powell, R., Reed, J., Wilch, T. & The Andrill-MIS Science Team, 2007, Sedimentology and stratigraphy of the AND-1B Core, ANDRILL McMurdo Ice Shelf Project, Antarctica. Terra Antartica, v. 14(3), p. 185-222.

Kyle, P.R., 1977, Mineralogy and glass chemistry of recent volcanic ejecta from Mt. Erebus, Ross Island, Antarctica, New Zealand Journal of Geology and Geophysics, v. 20, p. 1123-1146.

Kyle, P.R., 1981, Glacial history of the McMurdo Sound area, as indicated by the distribution and nature of McMurdo volcanic rocks in the Dry Valley Drilling Project, *in* McGinnis, L.D., ed., Dry Valley Drilling Project. Antarctic Research Series, v. 33, American Geophysical Union, Washington D.C., p. 403-412.

Kyle, P.R., 1990, McMurdo volcanic group-western Ross Embayment, Introduction, *in* LeMasurier, W.E., and Thomson, J.W., eds., Volcanoes of the Antarctica Plate and Southern Oceans, American Geophysical Union, Washington, D.C., p. 19-25.

Kyle, P.R., Moore, J.A. and Thirwall, M.F., 1992, Petrologic evolution of anorthoclase phonolite lavas at Mt. Erebus, Ross Island, Antarctica, Journal of Petrology, v. 33, p. 849-875

Kyle, P.R. and Muncy, H.L., 1989, Geology and geochronology of McMurdo Volcanic Group rocks in the vicinity of Lake Morning, McMurdo Sound, Antarctica: Antarctic Science, v. 1, p. 345–350.

Lorenz, V., 1974, Studies of the Surtsey tephra deposits, Surtsey Research Progress Report, v. 7, p. 72-79.

Machado, F., Parsons, W.H., Richards, A.F. and Mulford, J.W., 1962, Capelinhos eruption of Fayal volcano, Azores, 1957-1958, Journal of Geophysical Research, v. 67, p. 3519-3529.

Maicher, D., 2003, A cluster of Surtseyan volcanoes at Lookout Bluff, North Otago, New Zealand: Aspects of edifice spacing and time. *in* White, J.D.L, Smellie, J.L., and Clague, D.A., eds., Explosive Subaqueous Volcanism American Geophysical Union Monograph v. 140, American Geophysical Union, Washington D.C., p. 167-178.

Martin, U., and White, J.D.L., 2001. Depositional mechanisms of density current deposits from a submarine vent at the Otago Peninsula, New Zealand, *in* Kneller, B., Peakall, J., eds., Sediment Transport and Deposition by Particulate Gravity Currents, IAS Special Publication, Blackwell, Oxford, p. 245-261.

McIntosh, W.C., 2001, $^{40}Ar/^{39}Ar$ geochronology of tephra and volcanic clasts in CRP-2A, Victoria Land Basin, Antarctica, *in* Barrettm, P.J., Ricci, C.A. eds., Studies from the Cape Roberts Project, Ross Sea, Antarctica, Scientific Report of CRP-2/2A, Terra Antartica, v. 7(4), p. 621–630.

McKay, R., Browne, G., Carter, Carter, L., Cowan, E., Dunbar, G., Krissek, L., Naish, T., Powell, R., Reed, J., Talarico, F., and Wilch, T., 2009, The stratigraphic signature of Late Cenozoic oscillations of the Antarctic Ice Sheet in the Ross Embayment, Antarctica, Geological Society of America Bulletin, v. 121, 1537-1561.

Mueller, W.U., 2003, A subaqueous eruption model for shallow-water, small volume eruptions: Evidence from two precambrian examples, *in* White, J.D.L, Smellie, J.L., and Clague, D.A., eds., Explosive Subaqueous Volcanism American Geophysical Union Monograph v. 140, American Geophysical Union, Washington D.C., p. 189-203.

Mueller, W.U. and White, J.D.L., 1992,. Felsic fire-fountaining beneath Archean seas: pyroclastic deposits of the 2730 MA Hunter Mine Group, Quebec, Canada. Journal of Volcanology and Geothermal Research, v. 54, p. 117-134.

Mueller, W.U., Garde, A.A. and Stendal, H., 2000, Shallow-water, eruption-fed, mafic pyroclastic deposits along a Paleoproterozoic coastline: Kangerluluk volcano-sedimentary sequence, southeast Greenland, Precambrian Research, v. 101, p. 163-192.

Mueller, W.U., Dostal, J., and Stendal, H., 2002, Inferred Palaeoproterozoic arc rifting along a consuming plate margin: insights from the stratigraphy, volcanology and geochemistry of the Kangerluluk sequence, southeast Greenland: International Journal of Earth Sciences, v. 91, p. 209-230.

Naish, T.R., Powell, R.D., Barrett, P.J., Horgan, H., Dunbar, G., Wilson, G., Levy, R., Robinson, N., Carter, L., Pyne, A., Niessen, F., Bannister, S., Balfour, N., Damaske, D., Henrys, S., Kyle P.R. and Wilson, T., 2006, ANDRILL McMurdo Ice Shelf Project Scientific Prospectus, ANDRILL Contribution 4, Science Management Office, University of Nebraska-Lincoln, p. 1-18.

Naish, T.R., Powell, R.D., Levy, R., Henrys, S., Krissek, L., Niessen, F., Pompilio, M., Scherer, R., Wilson, G. & The ANDRILL-MIS Science Team, 2007, Synthesis of the Initial Scientific Results of the MIS Project (AND-1B Core), Victoria Land Basin, Antarctica, Terra Antartica, v. 14(3), p. 317-327.

Naish, T.R., Powell, R.D., Barrett, P.J., Levy, R.H., Henry, S., Wilson, G.S., Krissek, L.A., Niessen, F., Pompilio, M., Ross, J., Scherer, R., Talarico, F., Pyne, A., and the ANDRILL-MIS Science Team, 2008, Late Neogene climate history of the Ross Embayment from the AND-1B drill core: culmination of three decades of Antarctic margin drilling. In Cooper, A.K. (Ed.), Antarctica: A Keystone in a Changing World. Proceedings of the 10*th* International Symposium on Antarctic Earth Sciences. Washington, DC (The National Academies Press), p. 71-82.

Naish, T., Powell, R., Levy, R., Wilson, G., Scherer, R., Talarico, F., Krissek, L., Niessen, F., Pompilio, M., Wilson, T., Carter, L., DeConto, R., Huybers, P., McKay, R., Pollard, D., Ross, J., Winter, D., Barrett, P., Browne, G., Cody, R., Cowan, E., Crampton, J., Dunbar, G., Dunbar, N., Florindo, F., Gebhardt, C., Graham, I., Hannah, M., Hansaraj, D., Harwood, D., Helling, D., Henrys, S., Hinnov, L., Kuhn, G., Kyle, P., Läufer, A., Maffi oli, P., Magens, D., Mandernack, K., McIntosh, W., Millan, C., Morin, R., Ohneiser, C., Paulsen, T., Persico, D., Raine, I., Reed, J., Riesselman, C., Sagnotti, L., Schmitt, D., Sjunneskog, C., Strong, P., Taviani, M., Vogel, S., Wilch, T., and Williams, T., 2009, Obliquity-paced Pliocene West Antarctic Ice Sheet oscillations: Nature, v. 458, p. 322–328, doi:10.1038/nature07867.

Naish, T.R. and Wilson, G.S., 2009, Constraints on the amplitude of Mid-Pliocene (3.6–2.4 Ma) eustatic sea-level fluctuations from the New Zealand shallow-marine sediment record. Philosophical Transactions of the Royal Society A, p. 169-188 (doi:10.1098/rsta.2008.0223).

Pompilio, M., Dunbar, N., Gebhardt, A.C., Helling, D., Kuhn, G., Kyle, P., McKay, R., Talarico, F., Tulaczyk, S., Vogel, S., Wilch T., and The ANDRILL-MIS Science Team, 2007. Petrology and Geochemistry of the AND-1B Core, ANDRILL McMurdo Ice Shelf Project, Antarctica. Terra Antartica, v. 14(3), p. 255-288.

Rao, A., Chen, Y., Lee, S., Leigh, J., Johnson, A., Renambot, L., 2006, Corelyzer: Scalable Geologic Core Visualization using OSX, Java and OpenGL Apple's Worldwide Developers Conference 2006.

Ross, J. McIntosh, W.C., Dunbar, N. W., and ANDRILL-MIS Science Team Preliminary, 2007. ^{40}Ar/^{39}Ar results from the AND-1B core, *in* Cooper, A.K., Raymond, C.R. and the ISAES Editorial Team, eds., Antarctica: A Keystone in a Changing World–Online Proceedings of the 10th ISAES X, USGS Open-File Report, v. 1047, Extended Abstract 093.

Skilling, I.P., 1994, Evolution of an englacial volcano-Brown Bluff, Antarctica, Bulletin of Volcanology, v. 56, (6–7), p. 573-591.

Smellie, J.L. and Hole, M.J., 1997, Products and processes in Pliocene-Recent, subaqueous to emergent volcanism in the Antarctic Peninsula: examples of englacial Surtseyan volcano construction, Bulletin of Volcanology, v. 58, p. 628-646.

Smellie, J.L., 1999, Subglacial eruptions, *in* Sigurdsson, H., Houghton, B. F. McNutt, S. R., Rymer, H. and Stix, J., eds, Encyclopedia of Volcanoes, Academic Press, San Diego, p. 403-418.

Solgevik, H., Mattsson, H.B. and Hermelin, O., 2007, Growth of an emergent tuff cone: Fragmentation and depositional processes recorded in the Capelas tuff cone, São Miguel, Azores. Journal of Volcanology and Geothermal Research, v. 159(1), p. 246-266.

Song S.R. and Lo, H.J., 2002, Lithofacies of volcanic rocks in the central Coastal Range, eastern Taiwan: implications for island arc evolution, Journal of Asian Earth Sciences, v. 21, p. 23–38.

Stern, T.A., Davey, F.J. and Delisle, G., 1991, Lithospheric flexure induced by the load of the Ross Archipelago, southern Victoria Land, Antarctica, *in* Thomson, M.R.A., Crame, J.A. and Thomson, J.W., eds., Geological evolution of Antarctica, Cambridge University Press, p. 323-328.

Stix, J., and Gorton, M.P., 1989, Subaqueous volcanoclastic rocks of the Confederation lake area, Northwestern Ontario: discrimination between pyroclastic and epiclastic emplacement, Ontario Geological Survey Miscellaneous Paper, v. 143, p. 83-93.

Talarico, F. and Sandroni, S., 2009, Provenance signatures of the Antarctic Ice Sheets in the Ross Embayment during the Late Miocene to Early Pliocene: The ANDRILL AND-1B core record, Global and Planetary Change, v. 69, p- 103-123.

Thorarinsson, S., 1964. Surtsey. The new island in the North Atlantic, The Viking Press, New York, p. 47.

Walker, P.L., 1973. Lengths of lava flows. Philosophical Transaction of the Real Society of London, v. 274, p.107-118.

White, J.D.L., 1996. Pre-emergent construction of a lacustrine basaltic volcano, Pahvant Butte, Bulletin of Volcanology, v. 58, 4, p. 249-262.

White, J.D.L., 2000. Subaqueous eruption-fed density currents and their deposits. Precambrian Research, v. 101, p. 87-109.

White, J. D. L. and Houghton, B. F., 1999. Surtseyan and related eruptions. *in* Sigurdsson, H., Houghton, B. F. McNutt, S. R., Rymer, H. and Stix, J., eds, Encyclopedia of Volcanoes, Academic Press, San Diego, p. 495-512.

White, J.D.L. and Houghton, B.F., 2006, Primary volcaniclastic rocks, Geology, v. 34, p. 677-680.

Wilch, T. I.; McIntosh, W. C.; Panter, K. S.; Dunbar, N. W.; Smellie, J. L.; Fargo, A.; Scanlan, M.; Zimmerer, M. J.; Ross, J.; Bosket, M. E. 2008, Volcanic and Glacial Geology of the Miocene Minna Bluff Volcanic Complex, Antarctica, American Geophysical Union, Fall Meeting 2008, abstract #V11F-06.

Wilson, G., Damaske, D., Moeller, H.D., Tinto K. and Jordan, T., 2007a. The geological evolution of southern McMurdo Sound-new evidence from a high-resolution aeromagnetic survey, Geophysical Journal International, v. 170 , p. 93-100.

Wilson, G., Florindo, F., Sagnotti, L., Ohneiser, C. and the ANDRILL-MIS Science Team, 2007b. Paleomagnetism of the AND-1B Core, ANDRILL McMurdo Ice Shelf Project, Antarctica, Terra Antartica, 2007, v. 14(3), p. 289-296.

Wilson, G., Levy, R, Browne, G, Cody, R, Dunbar, N., Florindo, F., Henrys, S., Graham, I., McIntosh, W., McKay, R., Naish, T., Ohneiser, C., Powell, R., Ross, J., Sagnotti, L., Scherer, R., Sjunneskog, C., Strong, C.P., Taviani, M., Winter, D., and the ANDRILL-MIS Science Team, 2007c, Preliminary integrated chronostratigraphy of the AND-1B Core, Andrill McMurdo ice shelf project, Antarctica, Terra Antartica, v. 14(3), p. 297-316.

Wright A.C. and Kyle, P.R., A.15 Mount Bird. 1990a, *in* LeMasurier, W.E., and Thomson, J.W., eds., Volcanoes of the Antarctica Plate and Southern Oceans, American Geophysical Union, Washington, D.C., p. 97-98.

Wright A.C. and Kyle, P.R., A.16 Mount Terror. 1990b, *in* LeMasurier, W.E., and Thomson, J.W., eds., Volcanoes of the Antarctica Plate and Southern Oceans, American Geophysical Union, Washington, D.C., p. 99-102.

Zanon, V., Pacheco, J., Pimentel, A. 2008. Growth and evolution of an emergent tuff cone: considerations from structural geology, geomorphology and facies analysis of São Roque volcano, São Miguel (Azores), Journal of Volcanology and Geothermal Research, v. 180, 2-4, p. 277-291.

Figure Captions

Figure 1: Location of the core site and main geographical features of the Southern Erebus Volcanic Province. Map also shows volcanic centers (encircled with different colors) belonging to the Erebus volcanic province with relative time span of activity. Satellite image from SSEC/UW-Madison AWS Network.

Figure 2 : Stratigraphic summary of the AND-1B core between 500 and 800 m b.s.f.. Lithologies are plotted against depth.

Figure 3: Thin section optical (left column) and SEM backscattered images (right column) of selected representative samples of relevant facies in LSU5: A-A1: heterolithic epiclastic sandstones (facies 2-6); B-B1: volcanic tuff (facies 11a); C-C1: lava flow (facies 11b); D-D1: volcanic diamictites (facies 11c).

Figure 4: Composite stratigraphic log of LSU5A and LSU5B, showing facies distribution with depth. Lithologies are the same of Fig. 2.

Figure 5: Close up from Fig.1, illustrating the position of volcanic centers and glaci-volcaniclastic sediments relative to AND-1B core site, after Wilson et al. (2007).

Figure 6: Schematic models illustrating the progressive migration or growth of a volcanic edifice close to the coring site. Main eruptive, transport and depositional processes are also sketched (see

text for details); flow patterns are purely illustrative. VTC: volcanic-rich turbidity current; EFD: Eruption-fed density currents; VD: Volcanic diamictites; LF: Lava flows.

Figure 1
Click here to download high resolution image

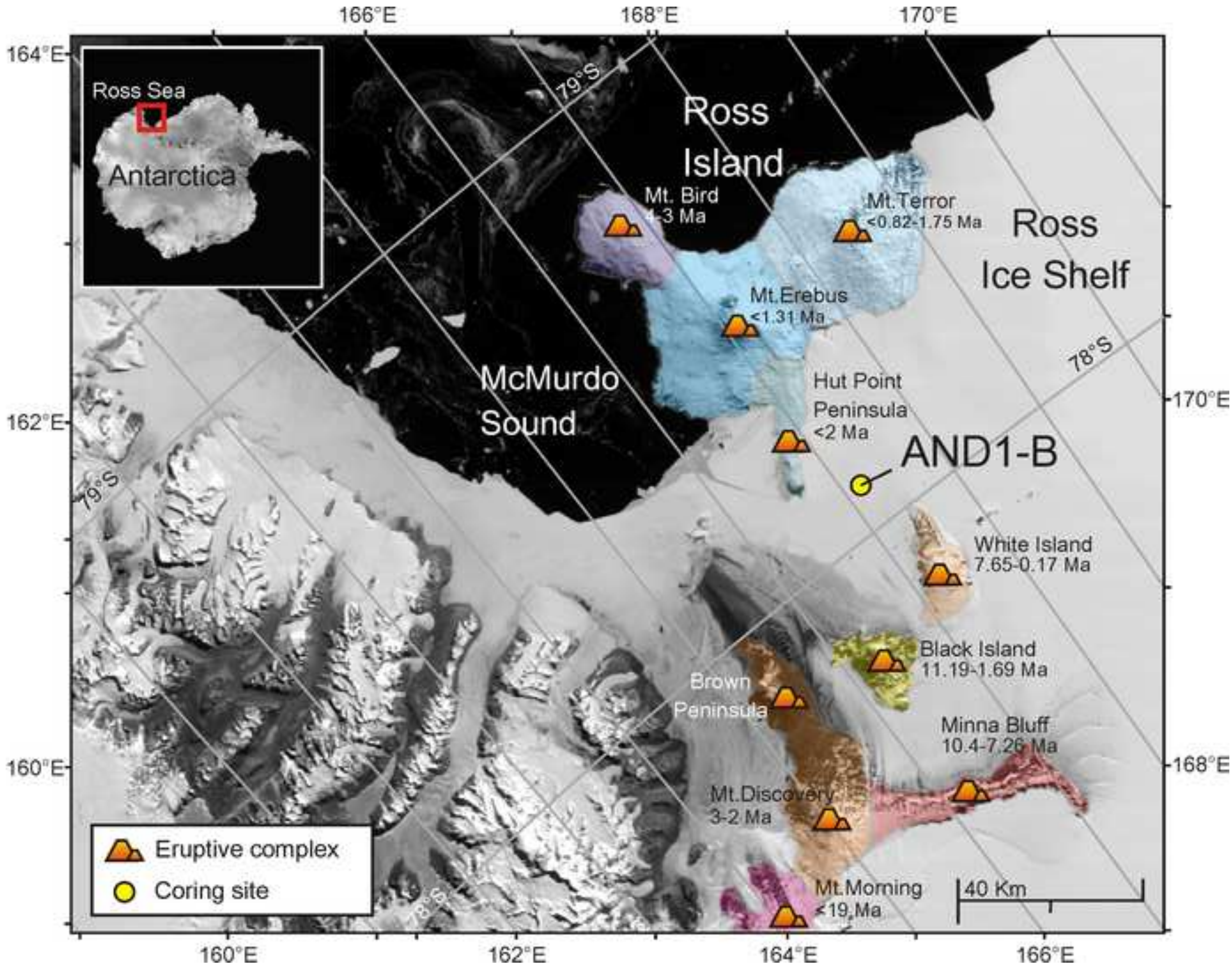

Figure 2
Click here to download high resolution image

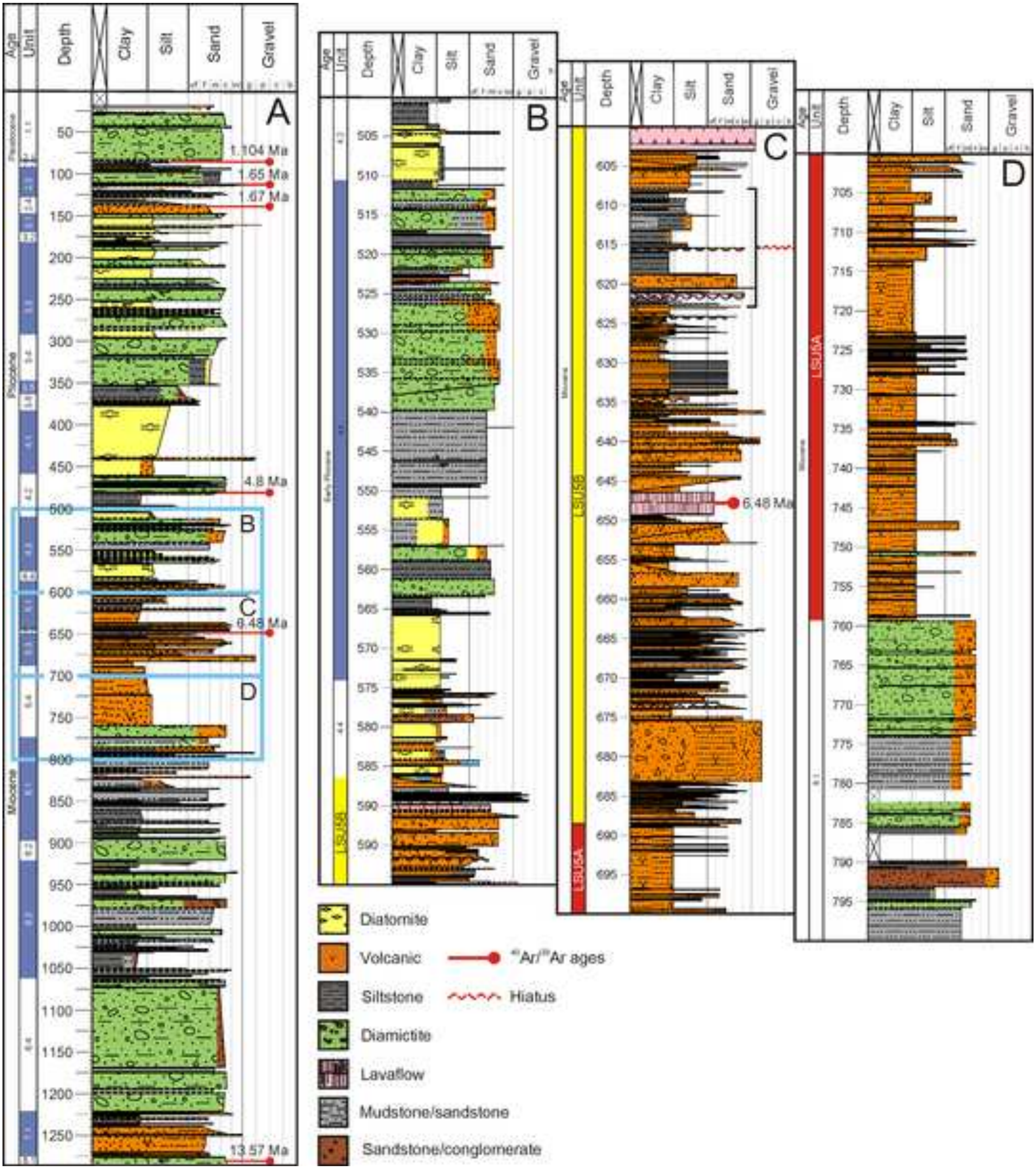

Figure 3

Click here to download high resolution image

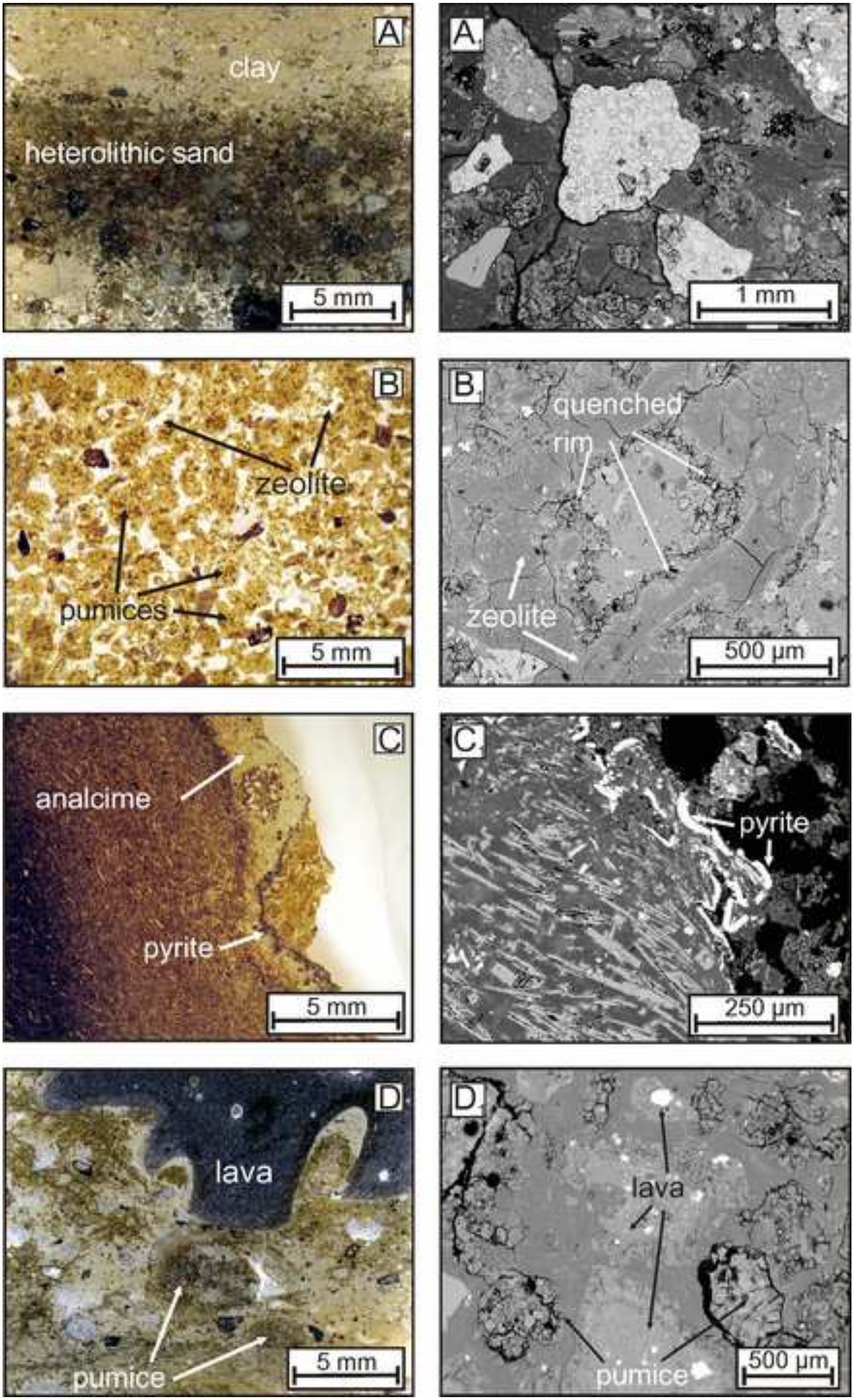

Figure 4

Click here to download high resolution image

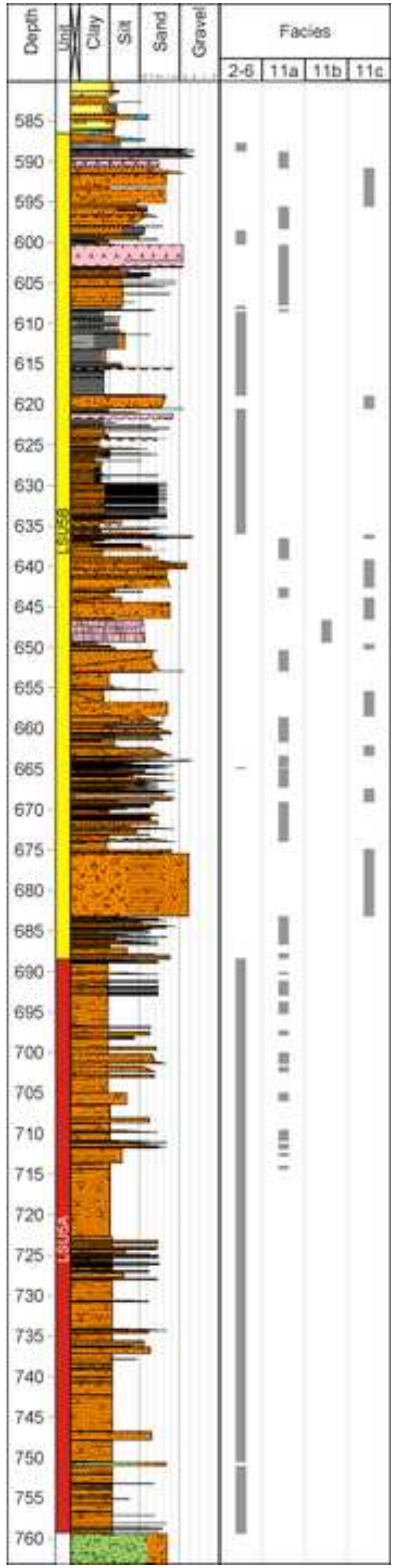

Figure 5
Click here to download high resolution image

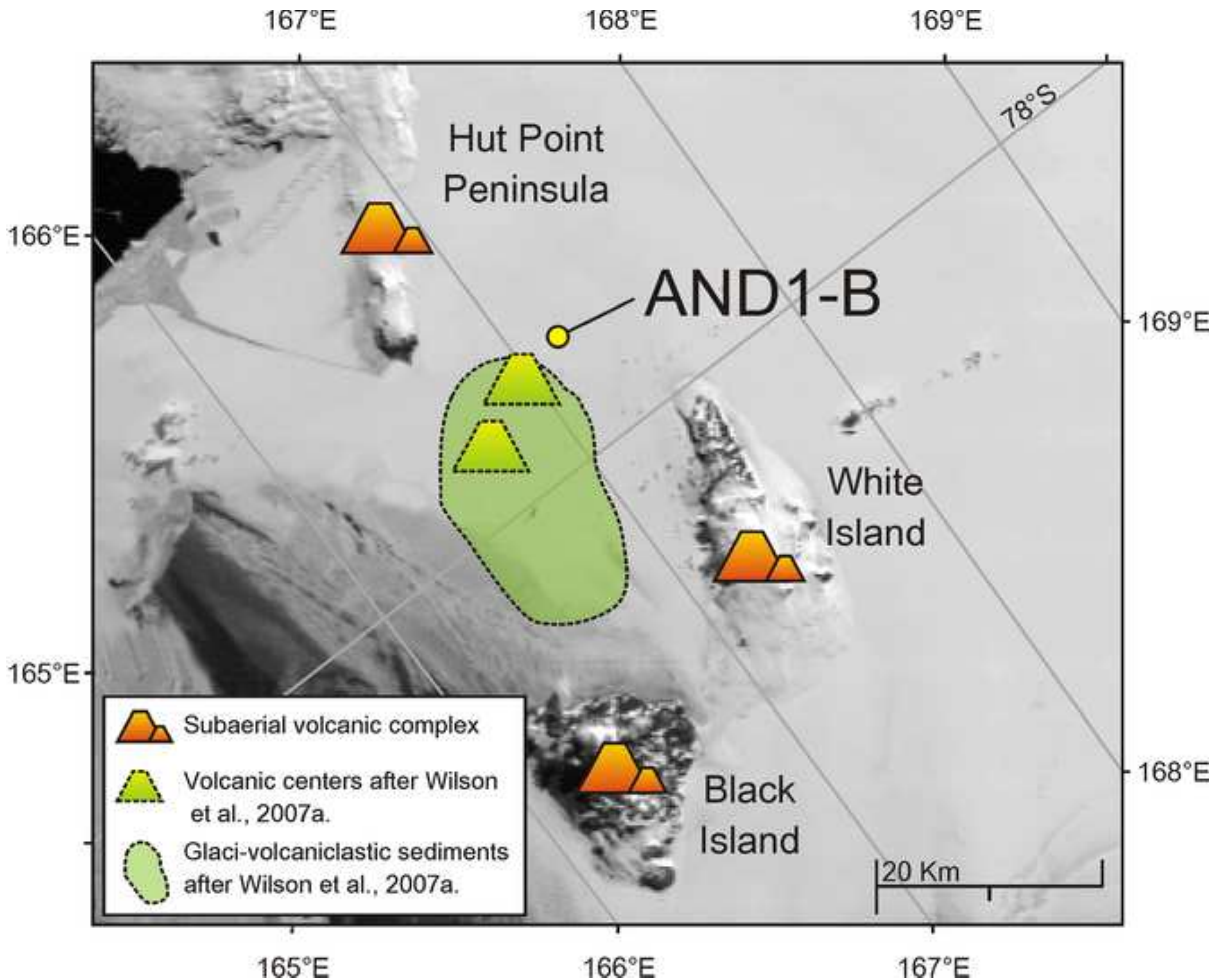

Figure 6
Click here to download high resolution image

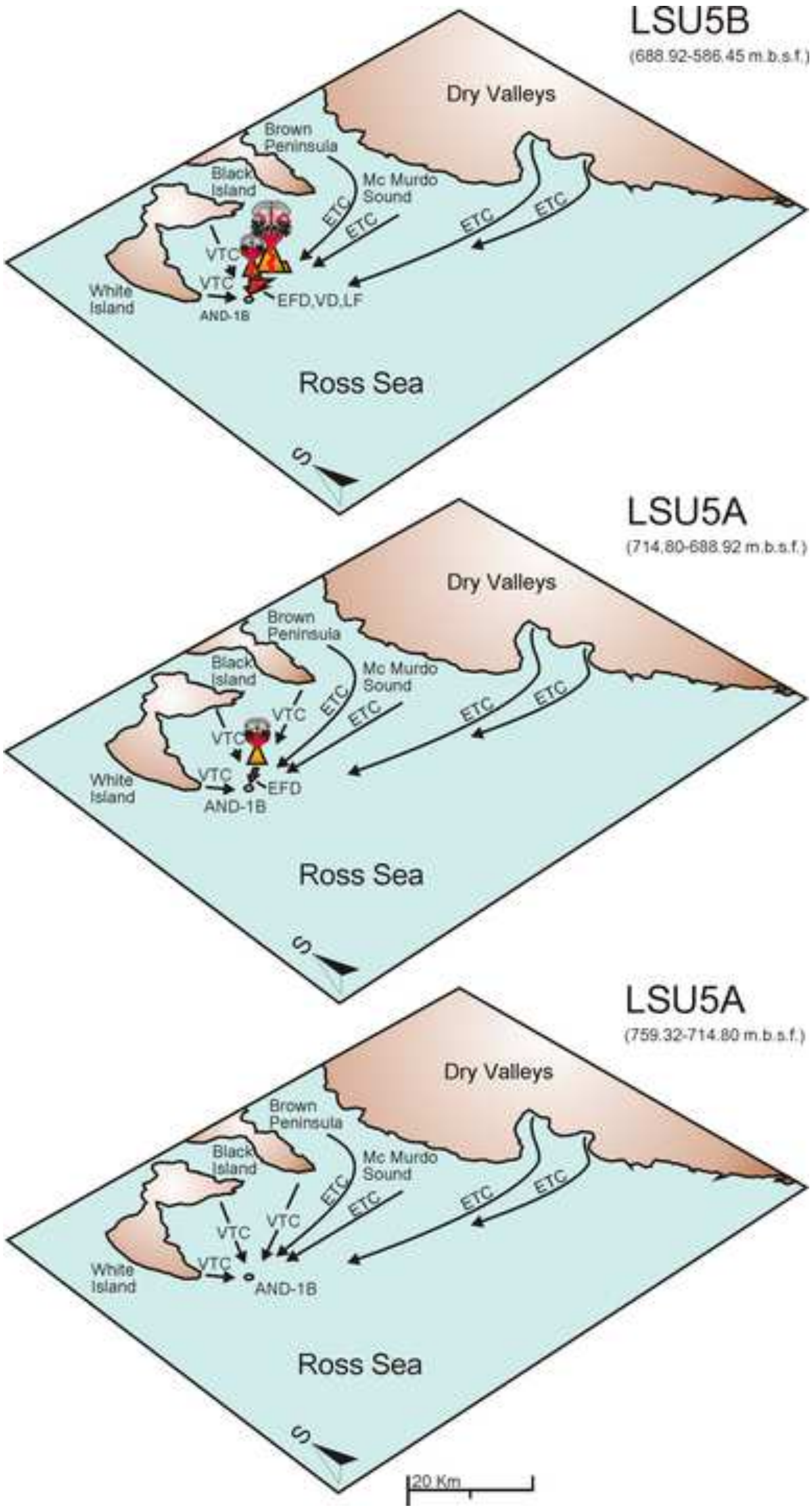

Table 1

TABLE 1. LITHOFACIES DESCRIPTION AND INTERPRETATION OF DEPOSITIONAL PROCESS

Facies	Bed description	Components	Volcanic/Glacial process
2 to 6 Volcanic-rich mudstone to sandstone	Cm- to mm-thick beds of siltstone, clayey siltstone, and fine to medium grained sandstone, interlaminated and interbedded at millimeter to centimeter scales (supplemental material 1)	Reworked glass shards, pumice and scoria, lava fragments, and magmatic crystals; granitoids, metasediments and mudstone intraclasts	Turbidity currents from a far located grounding
11a - Lapilli Tuff and Tuff	Cm- to dm-thick, massive to crudely stratified, coarse lapilli tuff to fine tuff, normally graded to well-bedded (supplemental material 2)	Pristine pumice, scoria and glass shards; few igneous crystals, and dense, angular lava fragments	High- to low-concentrated, eruption-fed, aqueous density current
11b - Lava Flow	Fine-grained tephrite (supplemental material 3)	N.A.	Submarine lava flow
11c - Volcanic Diamictite	Cm- to m-thick, coarse sand to breccia, massive to very poorly to faintly bedded (supplemental material 4)	Dense, angular lavas, scoria and oxidized altered volcanics	High-density mass flows (debris flows)

Supplemental file 1

Click here to download Supplemental file: supplemental material 1.tif

Supplemental file 2

Click here to download Supplemental file: supplemental material 2.tif

Supplemental file 3

Click here to download Supplemental file: supplemental material 3.tif

Supplemental file 4

Click here to download Supplemental file: supplemental material 4.tif

Supplemental file captions

Click here to download Supplemental file: Supplemental material captions.doc